RSC Advances

ROYAL SOCIETY OF CHEMISTRY

www.rsc.org/advances

Hydrogen peroxide sensitive hemoglobin-capped gold nanoclusters as a fluorescence enhancing sensor for the label-free detection of glucose

Fatemeh Molaabasi,[a] Saman Hosseinkhani,[b] Ali Akbar Moosavi-Movahedi [c] and Mojtaba Shamsipur,*[d]

In this paper, a novel label-free fluorescent detection system based on blue-emitting gold nanoclusters capped by hemoglobin (Hb-AuNCs) was designed as a fluorescence enhancing-quenching (on-off) sensor for the direct detection of low levels of glucose in serum samples. In the presence of glucose as a substrate and glucose oxidase (GOx) as catalyst, H_2O_2 is produced that can intensively enhance the fluorescence intensity of Hb-AuNPs. In the presence of hydrogen peroxide, an intramolecular electron transfer to Hb-AuNCs takes place under the heme degradation and/or iron release from Hb which is accompanied with the fluorescence enhancement of the nanoclusters. The DLS measurement, X-ray photoelectron spectroscopy patterns, and fluorescence and UV-visible spectra well supported this process. Upon the addition of H_2O_2, the fluorescence intensity enhanced linearly over the range of 0.5 μM to 700 μM with a limit of detection of 0.21 μM. The septic interaction of H_2O_2 with the sensing probe, allows it to develop a sensitive and selective glucose detection system by using glucose oxidase (GOx) with no need of complicated enzyme immobilization and any modification of the Hb-AuNCs. With this approach, the fluorescence quenching results in two linear dynamic ranges of 5 to 100 μM, and 100 to 1000 μM with a limit of detection of 1.65 μM for glucose detection. The designed fluorescent sensing system was then applied to the determination of H_2O_2 in two rain water samples and to five human serum samples for glucose detection. The Hb-AuNCs could be an effective candidate for new types of luminescence biosensors in the future, due to their fascinating features such as good water solubility, biocompatibility, excellent stability and potential applicability, and also to other H_2O_2-producing enzymatic reactions. In adsdition, the effective electron transfer between AuNCs and heme group of Hb in the presence of H_2O_2, makes the system promising for electrochemical applications.

[a] *Department of Chemistry, Tarbiat Modares University, Tehran, Iran.*

[b] *Department of Biochemistry, Faculty of Biological Sciences, Tarbiat Modares University, Tehran, Iran .*

[c] *Institute of Biochemistry and Biophysical Chemistry, University of Tehran, Tehran, Iran.*

[d] *Department of Chemistry, Razi University, Kermanshah, Iran.*

E-mail: mshamsipur@yahoo.com ; Fax: +98 21 66908030; Tel: +98 21 66906032

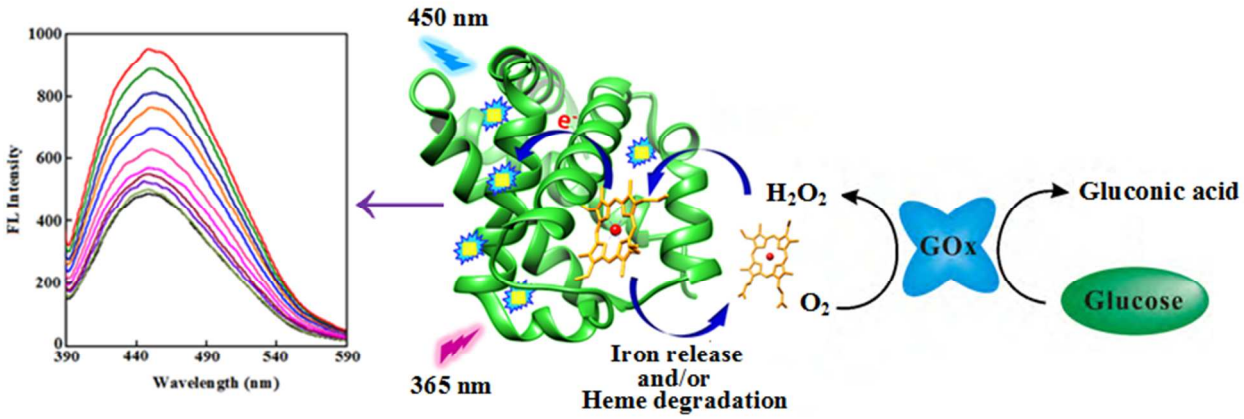

Introduction

Ultra-small noble metal nanoclusters (NCs), typically composed of several to a hundred metal atoms, present unique physical and chemical properties between atomic and nanoparticle behavior. They exhibit high quantum yield (QY), are photostable and, more importantly, are less affected by the stigma of toxicity often faced by luminescent quantum dots. Among metal nanoclusters, quantum-sized gold nanoclusters (AuNCs) have attracted an increasing research interest due to their unique electronic and optical properties as well as a wide range of potential applications, including catalysis, nanoscale biosensing, photonics, and drug delivery directly to the cell nucleus.[1,2] In addition, the emissions of AuNCs can be readily tuned from the UV to the near-IR region by varying their sizes, through control of the molar ratios of the reducing/capping agents to the metal ions and the nature of the capping agents.[3-9]

Proteins have shown to play an important role in directing the synthesis of functional nanomaterials under mild conditions because the amine, carboxyl, and thiol groups in proteins can serve as effective stabilizing agents in such formulations.[1,3,5,6,10] For example, the native bovine serum albumin (BSA) is applied to direct the synthesis of fluorescent Au_{25} clusters, which have been applied to the detection of various biologically important analytes based on different signal-transducing mechanisms.[3,10,11-16] In addition, the stabilities and fluorescence properties of AuNCs are dependent on the microenvironments provided by protein templates. It has demonstrated that some red AuNCs could be converted to blue emitters at pH 8 using BSA as a capping agent.[7]

The fact that the properties of AuNCs are highly dependent on the nature of protein templates, provided the opportunity to modulate the response patterns of protein capped AuNCs to a specific analyte simply by choosing some appropriate protein templates in nanocluster synthesis.[3,6,18] However, most of the current nanoclusters-based sensing systems are limited by their fluorescence quenching nature.[8,12,13,16,18-23] Such turn-off assays sometimes give false positive results, as the other quenchers or environmental stimulus might lead to fluorescence quenching.[24,25] To overcome this challenge while simplifying the operation process, for the first time, in this work we used an oxygen-transport metalloprotein, human adult hemoglobin (Hb), as an appropriate capping agent for AuNCs to prepare a label-free fluorescence enhancing probe for sensitive and selective detection of hydrogen peroxide and glucose.

Human adult hemoglobin (Hb), the major protein component in erythrocytes, exists as a tetramer of globin chains composed of two α and two β subunits, each of which possessing one redox iron heme group. Although Hb does not play a role as an electron carrier in biological systems, it has been shown to possess an enzyme-like catalytic activity. It is also an ideal model molecule for the study of direct electron transfer reactions of enzymes because of such unique structure.[26,27] With respect to the presence of heme group as the activity center in hemoglobin-capped gold nanoclusters (Hb-AuNCs), the protein can generate multifunctional nanoclusters by integrating the functioning of the biomolecules and nanoclusters. To our knowledge, there is no previous report on a non-aggregation sensor for the determination of H_2O_2 based on the signal amplification effect of catalyzing H_2O_2 to reduce the AuNCs probe. The fluorescence intensity of the Hb-AuNCs was found to enhance due to photoinduced intramolecular electron transfer between the heme group as donor and AuNCs as acceptor in the presence of H_2O_2, indicating that Hb remains active and enables the catalytic reaction between Hb-AuNCs and H_2O_2 (see Scheme 1).

Detection and estimation of glucose level in human serum, specifically with diabetes, is very important and has been widely investigated.[28] In biochemical analysis, glucose is mainly measured by monitoring H_2O_2 being stoichiometrically produced during its oxidation by dissolved oxygen in the presence of enzyme glucose oxidase (GOx),[19,20,28,29-31] emphasizing the fact that H_2O_2 is an important yardstick for glucose determination. Hydrogen peropxide is also a by-product in the oxidation metabolic process, which is harmful to the organism and causes damage to the body when its concentration reaches 0.5 mM. Moreover, since H_2O_2 is the most efficient oxidant for the conversion of dissolved sulfur dioxide (SO_2) to sulfuric acid (H_2SO_4), determination of H_2O_2 in rainwater can provide good amount of information about the environment.[32-34] Thus, it is still urgent to develop new approaches for determination of glucose and H_2O_2 with high sensitivity, low toxicity, and easy operation. In this paper, highly fluorescent Hb-capped AuNCs were synthesized, characterized and utilized as a fluorescence probe for selective detection of H_2O_2 and glucose. The fluorescence of Hb-AuNCs was found to enhance linearly by H_2O_2 in a certain concentration range, which was consequently used for the detection of low levels of glucose. The process of oxidation of glucose by glucose oxidase (GOx) and the subsequent fluorescence enhancing of the Hb-AuNCs by the resulting H_2O_2 is shown in Scheme 1.

(Scheme 1)

Experimental

Materials

All reagents used were of analytical grade and used without further purification. $HAuCl_4$ was obtained from Alfa Aesar (Ward Hill, MA, U.K.). $Li_2(SO_4)$, NaOH, NaCl, KCl, $MgCl_2$, $CaCl_2$, ascorbic acid, ammonium persulfate, sodium hypochlorite, hydrogen proxide and glucose oxidase were obtained from Merck (Darmstadt, Germany). Sodium borohydride ($NaBH_4$), L-cysteine, glutathion, fructose, galactose, lactose, maltose, manose, sacarose and glucose were purchased from Sigma-Aldrich Chemical Co. (St. Louis, MO). All stock solutions were prepared using deionized water having a resistivity of no less than 18 MΩ·cm (Milli-Q, Bedford, MA). The experimental procedures and protocols for preparation of hemoglobin were done according to the method of William and Tsay.[35] The concentration of the protein was determined by the method of Antonini and Brunori (ε_{415nm} = 125 mM^{-1} cm^{-1} or ε_{541nm} = 13.8 mM^{-1} cm^{-1} per heme). The concentrations were high enough (i.e., ≥100 μM) to avoid the formation of a considerable amount of dimers, which should always be ≤5%.[36,37]

Apparatus

Spectrofluorimetric measurements were performed using a Perkin-Elmer LS-50B fluorescence spectrometer (Perkin-Elmer, U.K.), equipped with a xenon lamp as excitation source. The emission spectra were recorded over the wavelength range of 390–600 nm upon excitation at 365 nm at a scan rate of 1500 nm min^{-1}. The spectral bandpass was set at 15 and 20 nm for excitation and emission, respectively. UV/Vis absorption spectra were recorded on a Model Scinco UV S-2100 (Cinco, Korea), using a 1.0 cm quartz cuvette, over the wavelength range from 250 to 800 nm.

Transmission electron microscopy (TEM) images were recorded using a Philips CM30 transmission electron microscope with an accelerating voltage of 150 kV. Samples were

prepared by drop casting solution on carbon coated copper grids and dried at room temperature. The X-ray photoelectron spectroscopy (XPS) studies were performed with an ESCALab220I-XL spectrometer (VG company, U.K.), and an Al Ka X-ray was used as the excitation source (hν = 1486.6 eV) for the XPS measurements. The spectrometer was configured to operate at high resolution with pass energy of 20 eV. The overall resolution was 1 eV for the XPS measurements. The core level binding energies (BE) were aligned with the adventitious carbon binding energy of 285 eV.

All pH measurements were performed using a Metrohm 713 pH/ion-meter with a standard uncertainty of 0.1 mV (Metrohm, Switzerland). The hydrodynamic sizes and the surface charges of the nanoparticles in aqueous solution in the absence and presence of H_2O_2 were measured using a Zetasizer nano ZS series dynamic light scattering (DLS) (Malvern Instruments Ltd., U.K.).

Synthesis of hemoglobin-capped AuNCs

All glassware were thoroughly cleaned with aqua regia (HNO_3/HCl, 1:3) and rinsed extensively with ethanol and ultrapure water. Hb-capping AuNCs were synthesized by chemical reduction of $HAuCl_4$ with hemoglobin. Briefly, aqueous $HAuCl_4$ solution (5 mL, 2.8 mM, 37 °C) was reacted with human adult hemoglobin (Hb) solution (5 mL, 28 mg mL^{-1}, 37 °C) under vigorous stirring. Ten minutes later, NaOH solution (1.0 mL, 1 M) was introduced to trigger the reduction of Au ions and subsequent formation of Au nanoclusters. The solution Au_8-Hb with a blue fluorescence emission changed from wine red to blackish green color after a few minutes. Finally, after 24 h reaction at 37 °C, the blackish green solution of Au nanoclusters was collected for characterization. In order to remove any suspended particles and byproducts with larger particle sizes, the as-prepared Hb-AuNCs containing some AuNCs was centrifuged (12,000 rpm, 10 min, 4 °C). In order to obtain a high concentration of gold nanoclusters, it is crucial to control parameters such as the molar ratios of the reducing/capping agents and pH value (~12.40 ± 0.03).

The absorption (a) and emission (b) spectra of nanoclusters are shown in Fig. 1A. The fluorescence emission maximum appeared at 450 nm and the absorption peaks centered at ~350 and 400 nm without any characteristic surface plasmon band of larger Au nanoparticles at around 520 nm.[8,38] The fluorescence property of the exposed solution did not decrease in terms of

intensity as well as peak position for more than 3 months. Therefore, the robust species in solution are thermodynamically stable and kinetically inert with respect to fluorescence property. The concentration of the AuNCs was 5.5 $\times 10^{-5}$ M. The photoluminescence full width at half-maximum was about 51 nm for AuNCs. As shown in Fig. 1B, the transmission electron microscope (TEM) image also suggested that the AuNCs have a narrow size distribution. The average size of Au nanoclusters in Hb molecules was estimated as 2.5 ± 0.6 nm. The final solution was stored at 4 °C until required for further use.

(Fig. 1)

Fluorescence measurements

In a typical experiment, 100 μL of as-prepared Au nanoclusters solution was diluted with phosphate buffer solution (10 mM, pH 7.4) and titrated by successive additions of H_2O_2 solution to give a final concentration of 100 μM. After addition of each portion of the H_2O_2 solution, this mixture was incubated at 37 °C for 30 min and then the fluorescence intensities were measured with an excitation wavelength of 365 nm and emission wavelengths in the interval of 390-600 nm. Based on these measurements, a linear correlation between the fluorescence intensity and H_2O_2 concentration was established.

Rainwater samples were collected from Tehran and Rasht cities in three different glass beakers (0.5 L) and were filtered through a 0.22 μm filter before the analysis of their H_2O_2 content. For the analysis of the two rainwater samples, 2.275 mL of the sample was mixed with 0.125 mL PBS buffer solution (10 mM, pH 7.4), followed by rapid addition of 100 μL Hb-AuNCs. The rainwater samples were then spiked with standard H_2O_2 solution (from 0 to 700 μM) and the fluorescence was measured after a reaction time of 30 min.

For glucose analysis, a mixture containing 250 μL of glucose solutions with different concentrations and 250 μL of 0.6 mg mL^{-1} GOx was first incubated at 37 °C for 10 min, and then the mixture was added to the diluted Hb-AuNCs and incubated for 30 min. The result obtained under these conditions indicated that the Hb-AuNCs sensor based on AuNCs possesses a good performance.

The glucose content of 5 different fresh serum samples, supplied by local clinical laboratories, was assessed by the proposed sensor as follows. A certain volume of serum samples (5-10 μL) and 1000 μL of 0.6 mg mL^{-1} GOx were incubated at 37 °C for 10 min. Then, 500 μL of above solution was added into 2000 μL of a phosphate buffered solution (10 mM, pH 7.4) of Hb-AuNCs and incubated for another 30 min, and the assay procedure was followed. The results were then compared with those obtained with a commercial glucose assay kit. In order to eliminate any matrix effects, the increase of photoluminescence intensity of the serum samples in the absence and presence of GOx was measured, and compared with the standard curve. Each experiment was repeated for three times and the experimental data were averaged to ensure the reproducibility. The serum samples, received from the laboratory, were stored in at 4 °C before use.

Results and discussion

Optimization of fluorescence sensing conditions for H_2O_2

The Hb-capped AuNCs exhibits remarkable enhancing fluorescence upon interaction with hydrogen proxide due to the presence of heme group as the activity center in hemoglobin. Before investigation of the effects of the concentrations of H_2O_2 on the fluorescence enhancement efficiencies, some experiments were carried out to optimize the sensing conditions such as the effects of solution pH, temperature, and reaction time.

Since the surface charge of proteins used as capping agent arises from ionization of the acidic and basic side chains of their amino acids,[39] we first investigated the influence of solution pH on the fluorescence response of Hb-AuNCs in the absence and presence of H_2O_2, and the results are shown in Fig. 2A. As seen, the fluorescence intensity of 2.2 μM of Hb-AuNCs both in the absence (a) and presence (b) of 1.0 mM of H_2O_2 increased with increasing pH of solution until a pH of 7.4 is reached, while further increase in pH from 7.4 to 12.0 resulted in no significant change in fluorescence intensity of the sensing system. Considering the fact that the highest sensitivity of Hb-AuNCs probe is expected to reach at pH values greater than the pI value of Hb (i.e., 6.8), due to the negative charge of Hb that can stabilize the AuNCs at pH > pI, a pH of 7.4 was selected for further studies.[6,40] It should be noted that the use of a probe solution

with no H_2O_2 as a control experiment clarified the fact that, over the entire range of pH studied, it is solely the presence of hydrogen peroxide that is responsible for the enhanced fluorescence intensity of the probe.

Other key factors to be optimized are the temperature and time of the Hb-AuNCs sensing system, since both the initial fluorescence intensity in the absence of H_2O_2 and the fluorescence enhancement in the presence of H_2O_2 found to be dependent on incubation temperature and time. Thus, the influences of the temperature and time on the fluorescence intensity of the Hb-AuNCs probe in the absence and presence of H_2O_2 were then studied over the range of 27 to 77 ºC and the results are shown in Figs. 2B and 2C, respectively. As is obvious from Fig. 2B, the peak intensity of Hb-AuNCs solutions at 450 nm in the absence of H_2O_2 has a maximum at 27 ºC, and slightly decreases upon increasing solution temperature. Aggregation of the Hb-AuNCs as a result of increased collisions at higher temperatures seems to mainly contribute to the lower fluorescence intensity at higher temperatures.[40] It is interesting to note that the decrease in emission of AuNCs at elevated temperatures in the absence of hydrogen proxide (shown in Fig. 2B) was found to largely recover with lowering the solution temperature, which clarified the fact that some other mechanisms such as thermal degradation of Hb under the experimental conditions used cannot be involved in the observed trend.

Meanwhile, in the presence of 1.0 mM H_2O_2, the trend in the plot of F/F_0 for the Hb-AuNCs against time at different temperatures (Fig. 2C) reveals that the sensor showed better performance at higher temperatures, so that maximum intensity reaches at 67 ºC. Moreover, other experiments clearly revealed that both the initial rates and the final fluorescence intensity increased with increasing H_2O_2 concentration (results not shown here). Also, the clusters showed maximum variation in emission intensity within 30 min (Fig. 2C), so that an incubation time of 30 min was selected for further studies.

(Fig. 2)

Detection of H_2O_2 based on fluorescent Hb-capped Au nanoclusters

Fig. 3A shows the increased intensity of fluorescence of 100 μL Hb-AuNCs upon interaction with different concentrations of H_2O_2 in the range of 0.5-700 μM at 37 ºC in PBS of pH 7.4, for a

fixed interval time of 30 min. As seen, the resulting fluorescence is significantly enhanced with increasing concentration of H_2O_2 in solution. Fig. 3B shows the plot of the fluorescence intensity ratio F/F_0 as a function of the H_2O_2 concentration. As is obvious, the calibration curve possesses two linear ranges, one from 0.5 to 100 μM (F/F_0 = 0.006 [H_2O_2] + 1.054, R^2=0.994) and another from 100 to 700 μM (F/F_0 = 0.0002 H_2O_2] + 1.1287, R^2=0.983) with a limit of detection (LOD) of 0.21 μM, based on a signal-to-noise ratio of 3. This LOD is lower than or comparable to that for most of the previously reported fluorescent[19,20,41] and electrochemical sensors[42-45] for H_2O_2 detection (see Table 1). Although a more sensitive linear range and much lower detection limits can be obtained at higher temperatures (see, as an example, the corresponding calibration graph for the system at 67 °C with a limit of detection of 0.04 μM in Fig. S1), we eventually preferred that at physiological temperature of 37 °C.

The proposed method exhibited excellent reproducibility with relative standard deviations (RSD) of 1.08% and 2.36% for 5 replicate detections of 5.0 and 700 μM H_2O_2 at 37 ºC, respectively. The selectivity of the proposed fluorescence probe for the detection of H_2O_2 was checked by comparing its fluorescent intensity interference of a 100 μM of H_2O_2 with that for an equimolar amount of several possible interferences including glucose, some thiol compounds including cysteine (Cys), glutathione (GSH) and ascorbic acid (AA) and some alkai and alkaline earth metal ions Li^+, Na^+, K^+, Mg^{2+} and Ca^{2+} and ammonium persulfate and sodium hypochlorite (at 1 mM level), as strong oxidizing agents, and the results are shown in Fig. 3C. As clearly seen, the other compounds tested possess negligible interfering effects on hydrogen peroxide detection, under the optimized experimental conditions used. It should be noted that the reported concentrations of the two aminothiols Cys and GSH in serum samples are less than 50 μM.[19]

(Fig. 3), (Table 1)

The applicability of the proposed sensing system was assessed by its use for determination of H_2O_2, in two rainwater samples collected locally from Tehran and Rasht cities (Iran), and the results are summarized in Table 2. By application of a standard addition method, the prepared sensing probe provided a linear response to H_2O_2 in spiked samples at concentrations over the range 0-100 μM (y = 0.0064 x+1.0953; R^2=0.997) for Tehran rainwater

and 0-35 μM (y = 0.0074 x+1.0597; R^2 = 0.999) for Rasht rainwater. The Hb-AuNCs probe provided recoveries of 90.5-112.0 % (Table 2A).

(Table 2)

Label-free fluorescent detection of glucose in the presence of GOx using Hb-AuNCs

In the next step, we found that the Hb-AuNCs combined with GOx-catalyzed reaction can be applied to the simple and sensitive detection of glucose with high sensitivity and wide linearity**.** In biochemical analysis, glucose is mainly measured by monitoring H_2O_2 being stoichiometrically produced during its oxidation by dissolved oxygen in the presence of glucose oxidase (GOx), as shown in Eq. (1):[19,20,29-31]

$$O_2 + \text{Glucose} \xrightarrow{\text{GOx}} H_2O_2 + \text{Gluconic acid} \quad (1)$$

Based on this catalytic reaction, H_2O_2 is an important yardstick for glucose determination. The glucose detection was realized via two steps: first, production of H_2O_2 via oxidation of equimolar amount of glucose by GOx followed by glucose detection by the Hb-AuNCs sensing system. To achieve sensitive detection of glucose, some key factors that influence the glucose detection were studied. The results obtained clearly revealed that the optimal values of GOx concentration and incubation time are 0.6 mg mL^{-1} and15 min, respectively (see Fig. S2). Also, the activity of glucose oxidase (GOx) was found to be optimal at pH 7.4 and 37 °C.

Under the optimal conditions mentioned above, by using 0.6 mg mL^{-1} GOx in 10 mM PBS buffer of pH 7.4 at 37 ºC for 15 min, the fluorescence probe was applied to detect various concentrations of glucose in solution. As shown in Fig. 4A, the fluorescence intensity ratio (F/F_0) at 450 nm increased linearity upon increasing amount of glucose over two concentration ranges of 5 to 100 μM (F/F0= 0.001 [glucose] + 1.009, R^2 = 0.982) and 100 to 1000 μM (F/F0= 0.0002 [glucose] + 1.1287, R^2 = 0.983), the sensitivity of the second calibration curve at higher glucose concentration being lower than that of the first one. In fact, when the concentration of glucose is high, a large amount of generated sodium gluconate may react with Hb-AuNCs and decrease the reaction ability of hydrogen peroxide with nanoclusters and, consequently,

resulting in low fluorescence enhancing efficiency.[20] The limit of detection (LOD) for glucose was 1.65 μM (S/N = 3), which is lower than those reported by many other methods, including fluorescence quenching,[19,20,29,30,41,46,47] chemiluminescence,[48,49] fluorescence resonance energy transfer (FRET),[55] calorimetry,[50] amperometry[51,52] and cyclic voltammetry,[42] as summarized in Table 1. Moreover, the reagents used in this method are simple and the operation procedures for the analysis are very easy. Indeed, lower limit of detection can be achieved by performing the glucose determination at 67 ºC (see Fig S1).

In order to assess the possible analytical applications of the above-described method, the selectivity of the designed sensing system based on Hb-AuNCs fluorescence probe for glucose (1 mM) was checked by conducting several control experiments using 1 mM solutions of maltose, lactose, fructose, galactose, sucrose and mannose. As shown in Fig. 4B, none of the tested carbohydrates, caused a significant change in the fluorescence intensity at 450 nm, suggesting that the biosensors have good selectivity due to the specific GOx enzyme catalysis. It should be noted that the concentration of glucose in blood samples is higher than all other carbohydrates by a factor of 100-fold.[19] Therefore, a sensitive and selective glucose biosensor is fabricated based on Hb-AuNCs fluorescent probe via an enhancing fluorescence approach. In addition, based on the very low interfering effect of glucose on H_2O_2 determination (as shown in Fig. 3C), in the case of selective catalytic detection of glucose with GOx, even at a relatively high concentration of 1 mM, the amount of possibly unconverted glucose is so low that it cannot have any measurable interfering effect on glucose detection.

Moreover, the present method is expected to be more suitable for the future biological applications owing to its moderate detection condition and low toxic characteristic of AuNCs, relative to the previous reports.[29,33,46,55] Also, the proposed method for the preparation of AuNCs does not require complicated reactions and does not feature toxic reducing agents (e.g., $NaBH_4$).

(Fig. 4)

Detection of glucose in real serum samples

Diabetes is a rapidly growing problem worldwide, which is managed at the individual level by monitoring and controlling blood glucose levels to minimize the negative effects of the disease.[23]

Here, the proposed enzymatic method was evaluated by analyzing 5 different serum samples for blood glucose content and comparing the results with those obtained with a commercial glucose assay kit. The results are shown in Table 2B. Considering the low detection limit of sensing system and the normal glucose level in human serum, 5-10 μL of fresh human serum will be enough for glucose analysis without any sample preparation. Furthermore, any matrix and background effect can be eliminated through comparing the fluorescence intensity of the probe for serum samples in the absence and presence of the GOs enzyme. Evidently, glucose concentration determined using the current method was found to be in satisfactory agreement with the values provided by the local laboratory (Table 2B). Moreover, as is clear from Table 2, after adding 25 mM glucose to the sample solutions, the recoveries were found to be in the range of 94.0–110.8%. It thus proved that the Hb-AuNCs sensor is appropriate for the diagnosis of diabetes with respect to concentration ranges of glucose, which is in the range of 4-8 mM for healthy people and 2-30 mM for diabetes.[46]

Study of detection mechanism of H_2O_2 by Hb-AuNCs

The synthetic method for gold nanoclusters mentioned in this paper is based on wet chemistry, in which Hb with red color was employed as both a reducing agent and a capping agent in alkaline medium. Recently, many researchers have focused on the application of different noble metal nanoclusters for the development of sensory systems based on the changes in their fluorescence intensities because of the fluorescence resonance energy transfer (FRET), electron transfer (ET), or other interactions occurring at the NCs surface.[2,8,13-15,18-22,40,53]

In the present study we employed UV-vis spectroscopy, fluorescence, DLS and XPS analyses, to clarify the mechanism of H_2O_2 detection. The UV-vis spectra of 2.2 μM of the Hb-AuNCs, as a fluorescent label, in the absence (1) and presence of 1.0 mM hydrogen peroxide at different time intervals from 0 (2) to 90 min (12) are depicted in Fig. 5A. As is obvious, the Hb-AuNCs exhibited two absorption bands, centered at wavelengths of 350 and 400 nm, corresponding to the characteristic absorption of the AuNCs and porphyrin-Soret band of hemoglobin, respectively,[26,36,37] the intensity of both of which in the presence of H_2O_2 being significantly decreased with elapse of time. The decrease of the porphyrin-Soret band of hemoglobin at 400 nm after adding 1 mM of H_2O_2 (Fig. 5A) could be related to the heme

degradation and/or iron release from hemoglobin stabilizer.[54-56] In addition, the rate of this process was found to increase with elapse of time at different temperatures (Fig. 5B), which corresponded to the fluorescence enhancement of the nanoclusters (see Fig. 2C). Thus, it seems possible that a simultaneous slight aggregation is also occurred with increasing temperature, the contribution of which is so small that cannot compete significantly with the very large fluorescence enhancement contribution due to intramolecular electron transfer to the Au(I) component present in AuNCs.

Through monitoring the fluorescence intensity of the Hb-AuNCs and H_2O_2 reaction mixture, a small H_2O_2-induced fluorescence quenching of Hb-AuNCs 2 min after addition of H_2O_2 was observed, which was then followed by a sharp increase in fluorescence with elapse of time without any significant peak shifting from 450 nm (Fig. 5C). This observation is of importance, as it allows the development of a fluorescence enhancing sensor for determination of H_2O_2. It is evident that the AuNCs are not prone to aggregation to form larger aggregates, thus leading to the increasing of fluorescence.[11,19] This hypothesis was supported by the Zeta-potential and hydrodynamic diameter (HDD) determinations. The DLS results revealed that the HDDs of the Hb-AuNCs in the absence and presence of 1 mM H_2O_2 are almost the same, possessing an average diameter of about 5.6-6.5 nm (see Fig. S3). It should be noted that the apparent HDD of Hb-capped AuNCs is larger than the TEM diameter (~2.6 nm), due to the fact that DLS gives the size of solvent-swollen aggregates while TEM gives the size of dry particles. Also, only a slight increase in the Zeta potential from –18.2 mV (n=3) to -15.8 mV (n=3) before and after addition of H_2O_2 was observed. Thus, both HDD and Zeta potential results clearly suggested that the H_2O_2-induced fluorescence enhancing was not due to changes in particle size or surface charge of the Hb-AuNCs.[58,59]

To find out about the question if blue fluorescence at 450 nm might originate from the aromatic side groups in the amino acid residues of the protein (i.e., tryptophan, tyrosine and phenylalanine), 1 mM of H_2O_2 was added to a 2.2 μM Hb solution and the corresponding UV-Vis and fluorescence spectra were recorded with elapse of time up to 60 min (see Figs. S4A and S4B). It was found that the distinct absorption band at 410 nm, corresponding to the heme group, remained more or less unperturbed and the fluorescence at 450 nm was not increased significantly after addition of increasing concentrations of H_2O_2, indicating the absence of any contribution from the present aromatic side groups in this respect.[40] Moreover, to rule out about

any possible metal enhancement of the fluorescence, we prepared 10.0±0.7 nm gold nanoparticles (AuNPs) and found that the fluorescence of Hb at 450 nm only slightly enhanced in the presence of H_2O_2 and AuNPs (Fig. S4C). Thus, it was concluded that the fluorescence enhancement band at 450 nm cannot be attributed to metal enhanced intrinsic fluorescence of Hb in the presence of H_2O_2.[40] Consequently, if the globin is not a source for the fluorescence enhancement, it presumably results from the presence of heme group in hemoglobin stabilizer. To prove this hypothesis, we conducted a comparison experiment by employing BSA-AuNCs as a control probe, in which red emitting of AuNCs consisting of 25 gold atoms stabilized with BSA molecules.[3,57] As it is clearly seen from Fig. 5C, the addition of 1 mM H_2O_2 induced a decrease in the fluorescence peak intensity of BSA-AuNCs at 610 nm, whereas in the H_2O_2 analysis proposed in this work, an increase of the fluorescence peak intensity at 450 nm for Hb-AuNCs was observed (Fig. 5D).

(Fig. 5)

It has been well established that heme degradation and iron release takes place under certain conditions when Hb reacts with H_2O_2, two fluorescent compounds are produced during the reaction of oxyhemoglobin with H_2O_2.[54,56,57] These two compounds including ferrylhemoglobin (Hb-$Fe^{IV}O$) and oxoferrylhemoglobin (Hb*-$Fe^{IV}O$) possessed excitation wavelengths of 321 nm and 460 nm, respectively, with respective emission wavelengths of 465 nm and 525 nm. Also, the reaction of H_2O_2 with Hb results in the formation of dityrosine, which exhibits a strong fluorescence with excitation and emission wavelengths of 320 and 410 nm, respectively. Consequently, the observed fluorescence enhancement for Hb-AuNCs in the presence of H_2O_2 is not related to dityrosin because of the quite different excitation and emission wavelengths applied to the detection of H_2O_2.

In fact, in this case, the electron transfer is likely to occur to Au metal from superoxide $O_2^{\cdot-}$, prepared from the degradation of oxyHb in the presence of H_2O_2, as suggested by Nagababu, and Rifkind:[54]

$$HbO_2 + H_2O_2 \longrightarrow HbFe(VI)=O + H_2O \quad (2)$$

$$HbFe(VI)=O + H_2O_2 \longrightarrow Hb^{+} + O_2^{\cdot-} + H_2O \quad (3)$$

Thus, in this respect, XPS study was used to clarify changes in chemical state and electronic structure of the AuNCs in the absence and presence of H_2O_2 after drying the solution on a silicon wafer. As depicted in Fig. 6, XPS spectrum in the absence of H_2O_2 shows a Au 4f band at a binding energies of 84.2 and 87.9 eV assigned to $4f_{5/2}$ and $4f_{7/2}$, with a spin-orbit splitting of 3.7 eV, confirming the reduction of Au(III) to Au(0) valance state in the reaction medium.[6,59-61] A small shift in the Fermi level, probably due to reduced size, is noted.[11] The Au $4f_{7/2}$ binding energy (BE) spectrum could be deconvoluted into two components centered at Au(0) BE (83.7 eV) and Au(I) BE (84.8 eV). It was found that about 39.9% Au (I) exists at the surface of the Au core in the absence of H_2O_2 (A). Meanwhile, in the presence of 2.5 mM H_2O_2, about 23.0% of Au(I) is reduced to Au(0). Hence, this study confirms that the exposure of Au^{3+} leads to the formation of an Au^{1+}-protein complex, so that the gradual evolution of the clusters can be attributed to the reduction of Au^{1+}, which takes place when heme degradation and/or heme release occurs during the oxidation of Hb upon the addition of hydrogen peroxide.[11] Thus, based on the above mentioned observations, it can be concluded that the electron transfer is occurred to Au(I) units due to heme degradation and/or heme release during the oxidation of hemoglobin by hydrogen peroxide. The decrease in Au(I) component in the presence of H_2O_2 rules out the oxidation of AuNCs, which consequently may correlate with the increased intensity of the fluorescence at 450 nm.[10,20,41,62,63]

4. Conclusion

The present study has demonstrated that the presence of H_2O_2 increases the luminescence of the blue-emitting gold nanoclusters due to the Hb/heme structure associated with AuNCs, as a novel phenomenon. The DLS measurements, XPS patterns, fluorescence and UV−vis spectra and Zeta potential and hydrodynamic diameter (HDD) determinations accurately recorded this process. The heme group as the activity center in hemoglobin, which may act as both a reducing and a stabilizing agent, plays a key role in fluorescence enhancement. Although the sensing mechanism is not fully understood, it involves electron transfer to the Au(I) ions on the surfaces of the Hb-AuNCs and some possible changes of energy transfer, brought about upon the addition

of H_2O_2. This leads to an opposite response in comparison with previous studies and resulting in the development of a novel enhancing fluorescence sensor for sensitive and selective detection of hydrogen peroxide and glucose. Furthermore, we believe that this work provides new insights into the application of Hb-AuNCs probe to other assay designs based on electron transfer and energy transfer, using different nanoparticles such as near-infrared (NIR)-to-visible upconversion nanoparticles and quantum dots in both enzymatic and non-enzymatic detections. The photostability and the intrinsic large stokes shift of the proposed probe, the facile procedure, the lower degree of sample matrix interference, and good reproducibility of the probe may lead to its practical uses for determination of many other analytes, such as uric acid, lactate, glutamate, and cholesterol, when performed in conjunction with suitable enzymes.

References

1 L. Shang, S. Dong and G. Ulrich Nienhaus, Ultra-small fluorescent metal nanoclusters: Synthesis and biological applications, *Nanotoday*, 2011, 6, 401–418.

2 L. Li, H. Liu, Y. Shen, J. Zhang and J.-J. Zhu, Electrogenerated chemiluminescence of Au nanoclusters for the detection of dopamine, *Anal. Chem.*, 2011, 83, 661–665.

3 J. Xie, Y. Zheng, J. Y. Ying, Protein-directed synthesis of highly fluorescent gold nanoclusters, *J. Am. Chem. Soc.*, 2009, 131, 888–889.

4 C.-A. J. Lin, T.-Y. Yang, C.-H. Lee, S. H. Huang, R. A. Sperling, M. Zanella, J. K. Li, J.-L. Shen, H.-H. Wang, H.-I. Yeh, W. J. Parak and W. H. Chang, Synthesis, characterization, and bioconjugation of fluorescent gold nanoclusters toward biological labeling applications, ACS Nano, 2009, 3, 395–401.

5 C.-A. J. Lin, C.-H. Lee, J.-T. Hsieh, H.-H. Wang, J. K. Li, J.-L. Shen, W.-H. Chan, H.-I. Yeh and W. H. Chang, *J. Med. Biol. Eng.*, 2009, 29, 276-283.

6 P. L. Xavier, K. Chaudhari, P. K. Verma, S. K. Palc and T. Pradeep, Luminescent quantum clusters of gold in transferrin family protein, lactoferrin exhibiting FRET, *Nanoscale*, 2010, 2, 2769–2776.

7 J. Zheng, C. Zhang and R. M. Dickson, Highly fluorescent, water-soluble, size-tunable gold quantum dots, *Phys.l Rev. Lett*., 2004, 93, 1-4.

8 J.-a. Annie Ho, H.-C. Chang, W.-T. Su, DOPA-mediated reduction allows the facile synthesis of fluorescent gold nanoclusters for use as sensing probes forf ions, *Anal. Chem.* 2012, 84, 3246−3253.

9 A. Zhang, Y. Tub, S. Qin, Y. Li, J. Zhou, N. Chen, Q. Lu, B. Zhang, Gold nanoclusters as contrast agents for fluorescent and X-ray dual-modality imaging, *J. Coll. Interface Sci.*, 2012, 372, 239–244.

10 K. Chaudhari, P. L. Xavier and T. Pradeep, Understanding the evolution of luminescent gold quantum clusters in protein templates, *ACS Nano*, 2011, 5, 8816–8827.

11 M. Wang, Q. Mei, K. Zhang, Z. Zhang, Protein-gold nanoclusters for identification of amino acids by metal ions modulated ratiometric fluorescence, *Analyst*, 2012, 137, 1618–1623.

12 C. V. Durgadas, P. Sharmaand and K. Sreenivasan, Fluorescent gold clusters as nanosensors for copper ions in live cells, *Analyst*, 2011, 136, 933-940.

13 C. V. Durgadas,. P. Sharmaand K. Sreenivasan, Fluorescent gold clusters as nanosensors for copper ions in live cells, Analyst, 2011, 136, 933-940.

14 F. Samari, B. Hemmateenejad, Z. Rezaei and M. Shamsipur, A novel approach for rapid determination of vitamin B12 in pharmaceutical preparations using BSA-modified gold nanoclusters, *Anal. Methods*, 2012, 4, 4155–4160

15 K.-Yi Pu, Z. Luo, K.i Li, J. Xie and B. Liu, Energy transfer between conjugated-oligoelectrolyte-substituted POSS and gold nanocluster for multicolor intracellular detection of mercury ion, *J. Phys. Chem. C* 2011, 115, 13069–13075.

16 D. Cao, J. Fan, J. Qiu, Y.Tu and J. Yan, Masking method for improving selectivity of gold nanoclusters in fluorescence determination of mercury and copper ions, *Biosens. Bioelectron.*, 2013, 42, 47–50.

17 X. L. Guével, B. Hötzer, G. Jung, K. Hollemeyer, V. Trouillet and M. Schneider, Formation of fluorescent metal (Au, Ag) nanoclusters capped in bovine serum albumin followed by fluorescence and spectroscopy, *J. Phys. Chem. C* 2011, 115, 10955–10963.

18 Y.-H. Lin and W.-L. Tseng, Ultrasensitive sensing of Hg^{2+} and CH_3Hg^+ based on the fluorescence quenching of lysozyme type VI-stabilized gold nanoclusters, *Anal. Chem.*, 2010, 82, 9194–9200.

19 Y.-C. Shiang, C.-C. Huang and H.-T. Chang, Gold nanodot-based luminescent sensor for the detection of hydrogen peroxide and glucose, *Chem. Commun.*, 2009, 3437–3439.

20 T. Wen, F. Qu, N. B. Li and H. Q. Luo, Polyethyleneimine-capped silver nanoclusters as a fluorescence probe for sensitive detection of hydrogen peroxide and glucose, *Anal. Chim. Acta*, 2012, 749, 56-62.

21 A. M. P. Hussain, S. N. Sarangi, J. A. Kesarwani and S. N. Sahu, Au-nanocluster emission based glucose sensing, Biosens. Bioelectron., 2011, 29, 60-65.

22 L. Hu, S. Han, S. Parveen,Y. Yuan, Li. Zhang and G. Xu, Highly sensitive fluorescent detection of trypsin based on BSA-stabilized gold nanoclusters, Biosens. Bioelectron., 2012, 32, 297–299.

23 X. Mu, L. Qia, P. Dong, J. Qiao, J. Hou, Z. Nie and H. Ma, Facile one-pot synthesis of L-proline-stabilized fluorescent gold nanoclusters and its application as sensing probes for serum iron, Biosens. Bioelectron., 2013, 49, 249–255.

24 L. Yang, Q. Song, K. Damit-Og and H.Cao, Synthesis and spectral investigation of a turn-on fluorescence sensor with high affinity to Cu^{2+}, Sens. Actuators B, 2013, 176, 181-185.

25 J. Li, X. Zhong, H. Zhang, X. C. Le and J.-J. Zhu, Binding-induced fluorescence turn-on assay using aptamer-functionalized silver nanocluster DNA probes, *Anal. Chem.*, 2012, 84, 5170−5174.

26 H. Cheng, H. Liu, W. Bao and G. Zou, Studies on the interaction between docetaxel and human hemoglobin by spectroscopic analysis and molecular docking, J. Photochem. Photobiol. B, 2011, 105, 126–132.

27 A. S. Kumar, P. Gayathri, P. Barathi and R. Vijayaraghavan, Improved electric wiring of hemoglobin with impure-multiwalled carbon nanotube/nafion modified glassy carbon electrode and its highly selective hydrogen peroxide biosensing, J. *Phys. Chem. C*, 2012, 116, 23692−23703.

28 K. J. Cash and H. A. Clark, Nanosensors and nanomaterials for monitoring glucose in diabetes, *Trends Mol. Med.*, 2010, 16, 584-593.

29 M. Hua, J. Tiana, H.-Ti. Lua, L.-Xi. Weng and L.-H. Wanga, H_2O_2-sensitive quantum dots for the label-free detection of glucose, *Talanta*, 2010, 82, 997-1002.

30 K. Wannajuk, M. Jamkatokec, T. Tuntulani and B. Tomapatanaget, Highly specific glucose fluorescence sensing based on boronic anthraquinone derivatives via the GO enzymatic reaction, *Tetrahedron*, 2012, 68, 8899-8904.

31 V. Sanz, S. de Marcos and J. Galbán, A blood-assisted optical biosensor for automatic glucose determination, *Talanta*, 2009, 78, 846–851.

32 Z. H. Li, D. H. Li, K. Oshita and S. Motomizu, Flow-injection determination of hydrogen peroxide based on fluorescence quenching of chromotropic acid catalyzed with Fe(II), *Talanta*, 2010, 82, 1225-1229.

33 Y. Gao, G. Wang, H. Huang, J. Hu, S. M. Shah and X. Su, Fluorometric method for the determination of hydrogen peroxide and glucose with Fe_3O_4 as catalyst, *Talanta*, 2011, 85, 1075-1080.

34 G. Shan, S. Zheng, S. Chen, Y. Chen and Y. Liu, Detection of label-free H_2O_2 based on sensitive Au nanorods as sensor, *Coll. Surf. B*, 2013, 102, 327– 330.

35 R. C. William, Jr. and K. Y.Tsay, A convenient chromatographic method for the preparation of human hemoglobin, *Anal. Biochem.*, 1973, 54, 137–145.

36 F. C. Chilaka, C. O. Nwamba, A. A.Moosavi-Movahedi, Cation modulation of hemoglobin interaction with sodium n-dodecyl sulfate (SDS). I: Calcium modulation at pH 7.20, *Cell Biochem. Biophys.*, 2011, 60, 187–197.

37 C. O. Nwamba, F. C. Chilaka and A. A. Moosavi-MovahediCation, Modulation of hemoglobin interaction with sodium n-dodecyl sulfate (SDS). II: Calcium modulation at pH 5.0, *Cell Biochem. Biophys.*, 2011, 61, 573–584.

38 J. Zheng, J. T. Petty and R. M. Dickson, High quantum yield blue emission from water-soluble Au8 nanodots, *J. Am. Chem. Soc.*, 2003, 125, 7780–7781.

39 M. A. H. Muhammed, P. K. Verma, S. K. Pal, A. Retnakumari, M. Koyakutty, S. Nair and T. Pradeep, Luminescent quantum clusters of gold in bulk by albumin-induced core etching of nanoparticles: Metal ion sensing, metal-enhanced Lluminescence, and biolabeling, *Chem. Eur. J.*, 2010, 16, 10103 – 10112.

40 F. Wen, Y.a Dong, L. Feng, S.Wang, S. Zhang and X.Zhang, Horse radish peroxidase functionalized fluorescent gold nanoclusters for hydrogen peroxide sensing, *Anal. Chem.*,2011, 83, 1193–1196.

41 L. Jin, L. Shang, S. Guo, Y. Fang, D. Wen, L. Wang, J. Yin and S. Dong, Biomolecule-stabilized Au nanoclusters as a fluorescence probe for sensitive detection of glucose, *Biosens. Bioelectro.*, 2011, 26, 1965–1969.

42 L. Jia, J. Liu and H. Wang, Preparation of poly(diallyldimethylammonium chloride)-functionalized graphene and its applications for H_2O_2 and glucose sensing, *Electrochim. Acta*, 2013, 111, 411– 418.

43 H. Fan, S. Zhang, P. Ju, H. Su and S. Ai, Flower-like Bi_2Se_3 nanostructures: Synthesis and their application for the direct electrochemistry of hemoglobin and H_2O_2 detection, *Electrochim. Acta*, 2012, 64,171– 176.

44 J. B. Raoof, R. Ojani, E. Hasheminejad, S. Rashid-Nadimi, Electrochemical synthesis of Ag nanoparticles supported on glassy carbon electrode by means of p-isopropyl calix[6]arene matrix and its application for electrocatalytic reduction of H_2O_2, *Appl. Surf. Sci.*, 2012, 258, 2788– 2795.

45 X. Bian , K. Guo , L. Liao , J. Xiao, J. Kong , C. Ji and B. Liu, Nanocomposites of palladium nanoparticle-loaded mesoporous carbon nanospheres for the electrochemical determination of hydrogen peroxide, *Talanta*, 2012, 99, 256-261.

46 X. Li, Y. Zhou, Z. Zheng, X. Yue, Z. Dai, S. Liu and Z. Tang, Glucose biosensor based on nanocomposite films of CdTe quantum dots and glucose oxidase, *Langmuir*, 2009, 25, 6580–6586.

47 C. Ubuka, E. K. Yetimoğlu, M. V. Kahramana, P. Demirbilek and M. Firlak, Development of photopolymerized fluorescence sensor for glucose analysisSoner, Sens. Actuaturs B, 2013, 181, 187-193.

48 K. Zargoosh, M. Shamsipur, M. Qandalee, M. Piltan and L. Moradie, Sensitive and selective determination of glucose in human serum and urinebased on the peroxyoxalate chemiluminescence reaction of a new fluorophore, Spectrochim. Acta A, 2011, 81, 679-683.

49 K. Zargoosh, M. J. Chaichi, M. Shamsipur, S. Hossienkhani, S. Asghari and M. Qandale, Highly sensitive glucose biosensor based on the effective immobilization of glucose oxidase/carbon-nanotube and gold nanoparticle in nafion film andperoxyoxalate chemiluminescence reaction of a new fluorophore, *Talanta*, 2012, 93, 37-43.

50 X. Chen, J. Chen, F. Wang, X. Xiang, M. Luo, X. Ji and Z. He, Determination of glucose and uric acid with bienzyme colorimetry on microfluidic paper-based analysis devices, *Biosens. Bioelectron.*, 2012, 35, 363-368.

51 H. Razmi, R. Mohammad-Rezaei, Graphene quantum dots as a new substrate for immobilization and direct electrochemistry of glucose oxidase: Application to sensitive glucose determination, Biosens. Bioelectron., 2013, 41, 498-504.

52 J.-D. Qiu, J. Huang and R.-P. Liang, Nanocomposite film based on graphene oxide for high performance flexible glucose biosensor, Sens. Actuaturs B, 2011, 160, 287-294.

53 L. Zhang, J. Zhu, S. Guo, T. Li, J. L, and E. Wang, Photoinduced electron transfer of DNA/Ag nanoclusters modulated by quadruplex/hemin complex for the construction of versatile biosensors, *J. Am. Chem. Soc.*, 2013, 135, 2403−2406.

54 E. Nagababu and J. M. Rifkind, Formation of fluorescent heme degradation products during the oxidation of hemoglobin by hydrogen peroxide, Biochem. Biophys. Res. Commun., 1998 247, 592–596.

55 B. Hu, L.-P. Zhang, M.-L. Chen, M.-L. Chen and J.-H. Wang, The inhibition of fluorescence resonance energy transfer between quantum dots for glucose assay, *Biosens. Bioelectron.*, 2012, 32, 82-88.

56 E. Nagababu and J. M. Rifkind, Hemed during autoxidation of oxyhemoglobin, Biochem. Biophys. Res. Commun., 2000, 273, 839–845.

57 E. Nagababu , J. G. Mohanty , S. R. Ostera and J. M. Rifkind, Role of the membrane in the formation of heme degradation products in red blood cells, Life Sci., 2010, 86, 133-138.

58 L.-Y. Chen, C.-C. Huang, W.-Y. Chen, H.-J. Lin and H.-T. Chang, Using photoluminescent gold nanodots to detect hemoglobin in diluted blood samples, Biosens. Bioelectron., 2013, 43, 38-44.

59 M. P. Casaletto, A. Longo, A. Martorana,A. Prestianni and A. M. Venezia, XPS study of supported gold catalysts: the role of Au0 and $Au^{+\delta}$ species as active sites, *Surf. Interface Anal.*, 2006, 38, 215–218.

60 M. Behera and S. Ram, Spectroscopy-based study on the interaction between gold nanoparticle and poly (vinylpyrrolidone) molecules in a non-hydrocolloid, *Behera Ram Int. Nano Letters*, 2013, 17, 3-7.

61 Y. Do, J.-S. Choi, S. K. Kim and Y. Sohn, The interfacial nature of TiO_2 and ZnO nanoparticles modified by gold nanoparticles, *Bull. Korean Chem. Soc.*, 2010, 31, 2170-2174.

62 U. Anand, S. Ghosh and S. Mukherjee, Toggling between blue- and red-emitting fluorescent silver nanoclusters, *J. Phys. Chem. Lett.*, 2012, 3, 3605−3609.

63 P.-H. Li, J.-Y. Lin, C.-T. Chen, W.-R. Ciou, P.-H. Chan, L. Luo, H.-Y. Hsu, E. W.-G. Diau, and Y.-C. Chen, Using gold nanoclusters as selective luminescent probes for phosphate-containing metabolites, *Anal. Chem.*, 2012, 84, 5484−5488.

Figure Captions

Scheme 1. Schematic illustration for fluorescence turn-on detection of H_2O_2 based on intramolecular electron transfer between heme group and AuNCs in Hb-AuNCs.

Fig.1. (A) Absorption (a) and fluorescence (b) spectra (λ_{em} = 450 nm) of the Hb-AuNCs. (B) TEM image of the as-prepared Hb-AuNCs.

Fig.2. (A) pH dependence fluorescence intensity of Hb-AuNCs (2.2 μM) in the absence (a) and presence (b) 1 mM of H_2O_2 after 60 min. (B) Temperature dependence fluorescence intensity of Hb-AuNCs (2.2 μM) in the absence of H_2O_2 at different temperatures. (C) Time dependence response of the 2.2 μM Hb-AuNCs after addition of 1 mM H_2O_2 at different temperatures: (a) 27, (b) 37, (c) 47, (d) 57, (e)67, (f) 77 ºC.

Fig. 3. (A) Fluorescence spectra representing the enhancing effect of different concentrations of H_2O_2 on 2.2 μM Hb-AuNCs at 450 nm (λ_{ex} = 365 nm) in PBS buffer (10 mM, pH =7.4): (a) 0, (b) 0.5, (c) 1, (d) 3, (e) 5, (f) 10, (g) 25, (h) 50, (i) 75, (j) 100, (k) 200, (l) 500, (m) 700 μM. (B) Plot of fluorescence ratio (F/F_0) of the fluorescent Hb-AuNCs at 450 nm for different concentrations of H_2O_2 at 37 ºC; Inset shows the linear range from 0.5 to 100 μM; [Hb-AuNCs] = 2.2 μM; Error bars represent ±3σ. (C) Fluorescence enhancing effect [$(F-F_0)/F_0$] of 2.2 μM Hb-AuNCs at 450 nm ($\lambda_{ex.}$ = 365 nm) in PBS buffer (10 mM, pH =7.4,) in the presence of 100 μM H_2O_2 and potential interferences GSH, Cys, glucose, AA, Li^+, Na^+, K^+, Mg^{2+}, Ca^{2+}.

Fig. 4. (A) Plot of fluorescence ratio (F/F_0) of the fluorescent Au nanoclusters at 450 nm for different concentrations of glucose at 37 ºC. Inset shows the linear ranges from 5 μM to 100 μM; [Hb-AuNCs] = 2.2 μM and [GOx] = 0.6 mg mL^{-1}; error bars represent ±3σ. (B) Fluorescence enhancing effect [$(F-F_0)/F_0$] of 2.2 μM Hb-AuNCs at 450 nm (λ_{ex}= 365 nm) in PBS buffer (10 mM, pH =7.4,) in the absence (blue, left) and presence (red, right) of 0.6 mg mL^{-1} GOx for 1000 μM of different carbohydrates: glucose (1), sacarose (2), manose (3), maltose (4), lactose (5), galactose (6), fructose (7).

Fig. 5. (A) Absorption spectral changes of 2.2 μM Hb-AuNCs at 27 ºC (1) upon addition of 1 mM H_2O_2 as a function of time: (2) 2, (3) 4, (4) 6, (5) 8, (6) 12, (7) 24, (8) 36, (9) 48, (10) 60, (11) 72, (12) 90 min. (B) Normalized absorption variation at 400 nm as a function of time for 2.2 μM Hb-AuNCs after addition of 1 mM H_2O_2 at different temperatures: (1) 27, (2) 37, (3) 47, (4) 57, (5) 67 ºC. The time fluorescence response of the AuNCs upon addition of 1 mM H_2O_2 to 2.2 μM BSA-AuNCs (λ_{ex} = 370 nm) (C) and to 2.2 μM Hb-AuNCs (λ_{ex} = 365 nm) (D). Time response was from 0 to 60 min.

Fig. 6. XPS spectra of Au (4f) for 2.2 μM Hb-AuNCs in the absence (A) and presence of 2.5 mM H_2O_2 (B): (1) Hb-AuNCs, (2) fitting line, (3) Au(0) line, (4) Au(I) line

Table 1 Comparison of sensor platforms for the detection of hydrogen peroxide and glucose

Method	System	DLR	LOD (μM)	Ref.

Fuorescence quenching	11-mercaptoundecanoic acid-bound Au nanodots (11-MUA–Au NDs)	H_2O_2 : 100 nM–1.0 mM Glucose : 30 μM –1.0 mM	0.03 1.0	19
Fuorescence quenching	CdTe Quantum Dots / GOx	Glucose : 0.5-16 mM	500	46
Fuorescence quenching	Polyethyleneimine-capped silver nanoclusters (PEI-Ag NCs)	H_2O_2 : 0.5-100 μM Glucose : 1-1.0 mM	0.40 0.8	20
Fuorescence quenching	Bovine serum albumin-Au nanoclusters (BSA-Au NCs)	H_2O_2 : 1-100 μM Glucose : 100 μM-0.5 mM	0.3 5	41
Fuorescence quenching	CdTe/CdS quantum dots / GOx	Glucose : 1.8 μM – 1mM	1.8	29
Fuorescence quenching	Boronic acid anthraquinones/GOx	Glucose : 0.08-0.42 mM	11.4	30
Fluorescence quenching	The binding of phenylboronic acids with glucose diols in membrane including Vinylphenylboronicacid–hydroxyethylmethacrylate	Glucose : 0.278-5.56 mM	8.9	47
Chemiluminescence	Bis(2,4,6-trichlorophenyl)oxalate (TCPO) / H_2O_2 /Flu di(tert-butyl)-2-(tert-butylamino)-5-[(E)-2-phenyl-1-ethenyl]- 3,4-furandicarboxylate	Glucose : 2.5 μM-175 M	1.1	48
Chemiluminescence	Immobilization of GOx / carbon nanotubes /gold nanoparticles in nafion film on graphite support	Glucose : 2.25-175 μM	1	49
Fluorescence resonance energy transfer (FRET)	The inhibition of FRET between Green QDs-Con A as donors and Red QDs-NH2-glu as acceptors	Glucose : 0.1-2.0 mM	30	55
Colorimetry	bienzyme detection on microfluidic paper-based analysis devices (μPADs)	Glucose : 0.05-1 mM	38.1	50
Electrochemical (amprometry)	Graphen quantum dot (GQD)/GOx/modified carbon ceramic electrod	Glucose : 5-1270 μM	1.73	51
Electrochemical (amperometry)	Chitosan-ferrocen/ graphen oxide/ GOx/ modified GC electrode	Glucose : 0.02-6.78 mM	7.6	52
Electrochemical (cyclic voltametry)	poly(diallyldimethylammonium chloride)-graphene/GOx/ modified GC electrode	H_2O_2 : 0.04-139.42 Glucose : 0.02-1.8 mM	10 8	42
Electrochemical (amperometry)	Flower-like Bi_2Se_3 nanostructures/ hemoglobin/modified GC electrode	H_2O_2 : 2-100 μM	0.63	43
Electrochemical (amperometry)	Ag NPs/ p-isopropyl calix[6]arene/modified GC electrode	H_2O_2 : 0.05-6.5 mM	27	44
Electrochemical (amperometry)	palladium nanoparticle/ mesoporous carbon nanospheres/modified GC electrode	H_2O_2 : 7.5 μM-10 mM	1.0	45
Fuorescence enhancing	Hemoglobin-Au nanoclusters (Hb-AuNCs)	H_2O_2 : 0.5-700 μM Glucose : 5-1000 μM	0.21 1.65	This study

DLR = Dynamic linear range. LOD = Limit of detection.

Table 2 Results of recovery studies of H_2O_2 from rainwater samples (n=3) (A) and determination of glucose in the human serum samples (n=5) (B)

(A)

Rainwater Samples	Spiked amount (μM)	Found amount (μM)	Recovery (%)
Sample 1	0	8.9 ± 0.2	–
	5.0	13.8 ± 0.5	98.0 ± 5.9
	15.0	25.7 ± 0.6	112.0 ± 2.5
Sample 2	0	18.8 ± 1.7	–
	20.0	36.9 ± 2.0	90.5 ± 10.1
	40.0	63.3 ± 2.3	111.2 ± 5.7

(B)

Serum samples	Spiked amount (mM)	Found amount (mM)	Recovery (%)	Local laboratory (mM)
Sample 1	0	15.8 ± 1.1	–	16.4
	25.0	41.3 ± 1.2	102.0 ± 4.8	
Sample 2	0	13.2 ± 1.9	–	14.2
	25.0	39.2 ± 0.5	104.0 ± 1.9	
Sample 3	0	20.0 ± 1.1	–	21.1
	25.0	43.8 ± 0.7	95.2 ± 2.9	
Sample 4	0	9.0 ± 0.3	–	10.5
	25.0	32.5 ± 0.8	94.0 ± 4.5	
Sample 5	0	6.9 ± 0.3	–	6.6
	25.0	34.6 ± 1.3	110.8 ± 4.1	

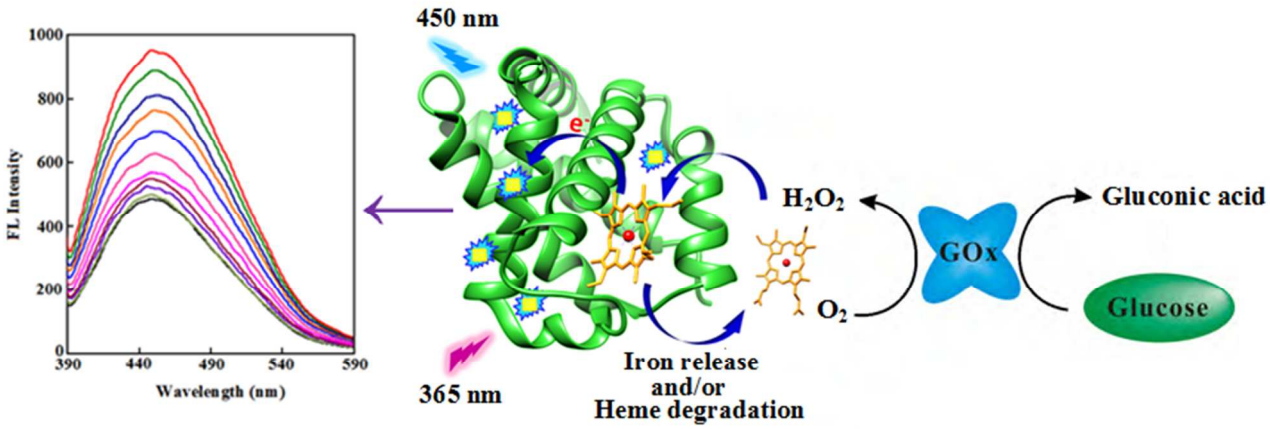

Scheme 1

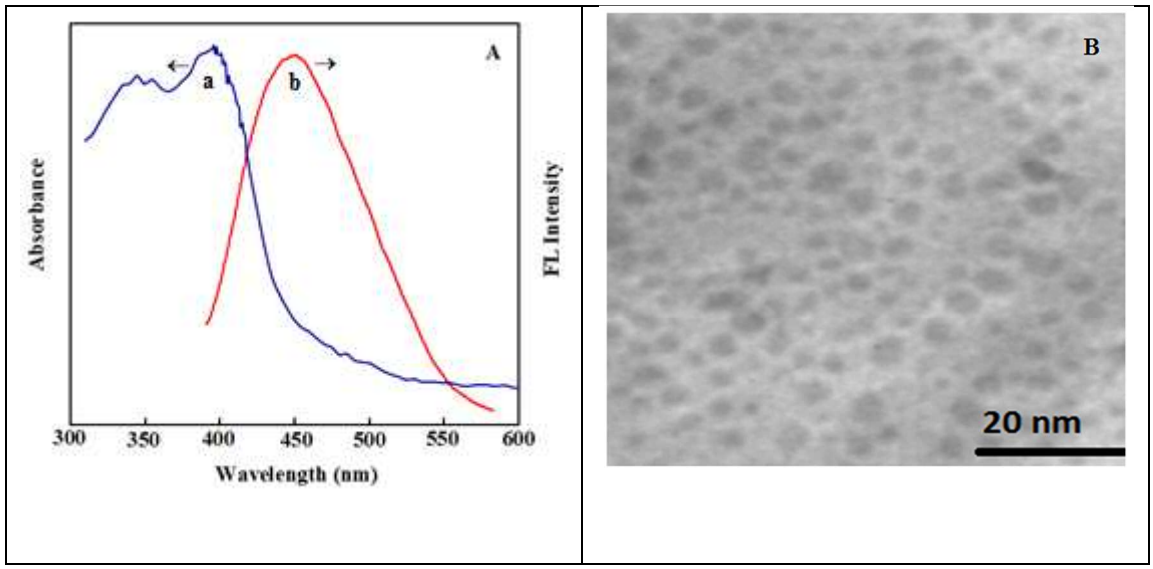

Fig. 1

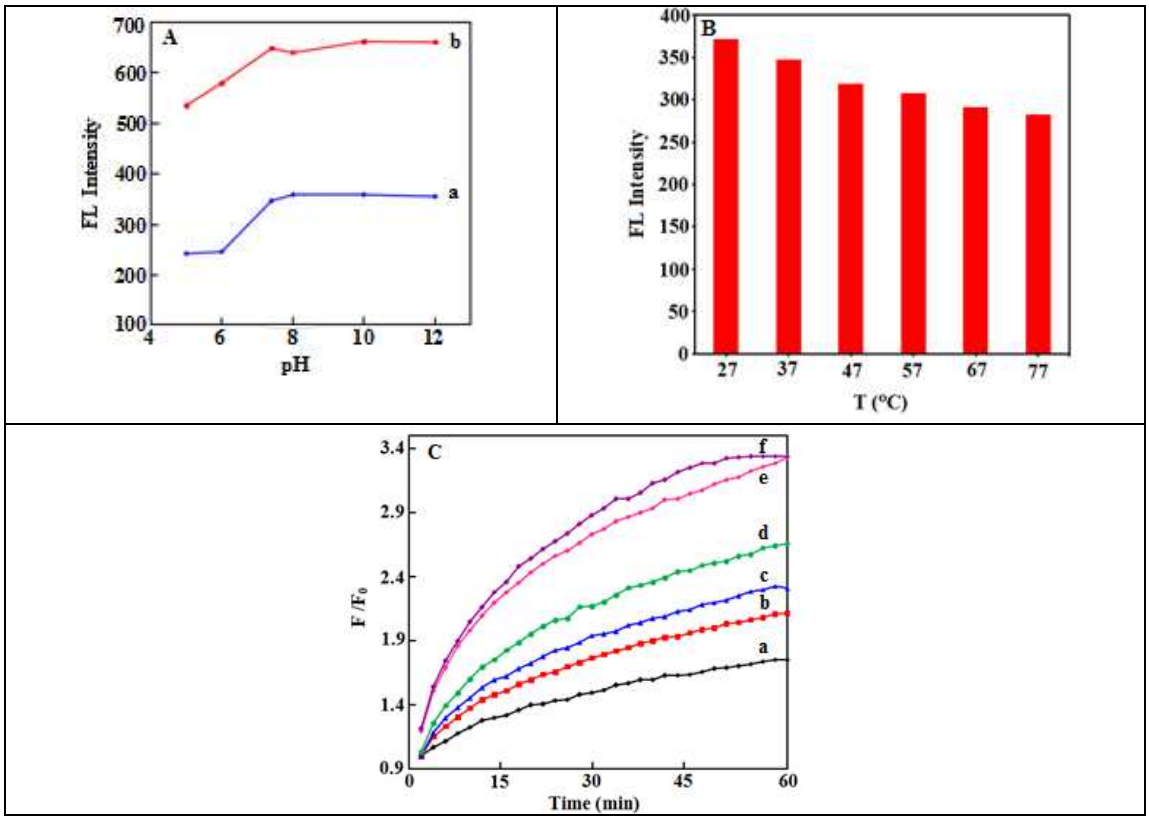

Fig. 2

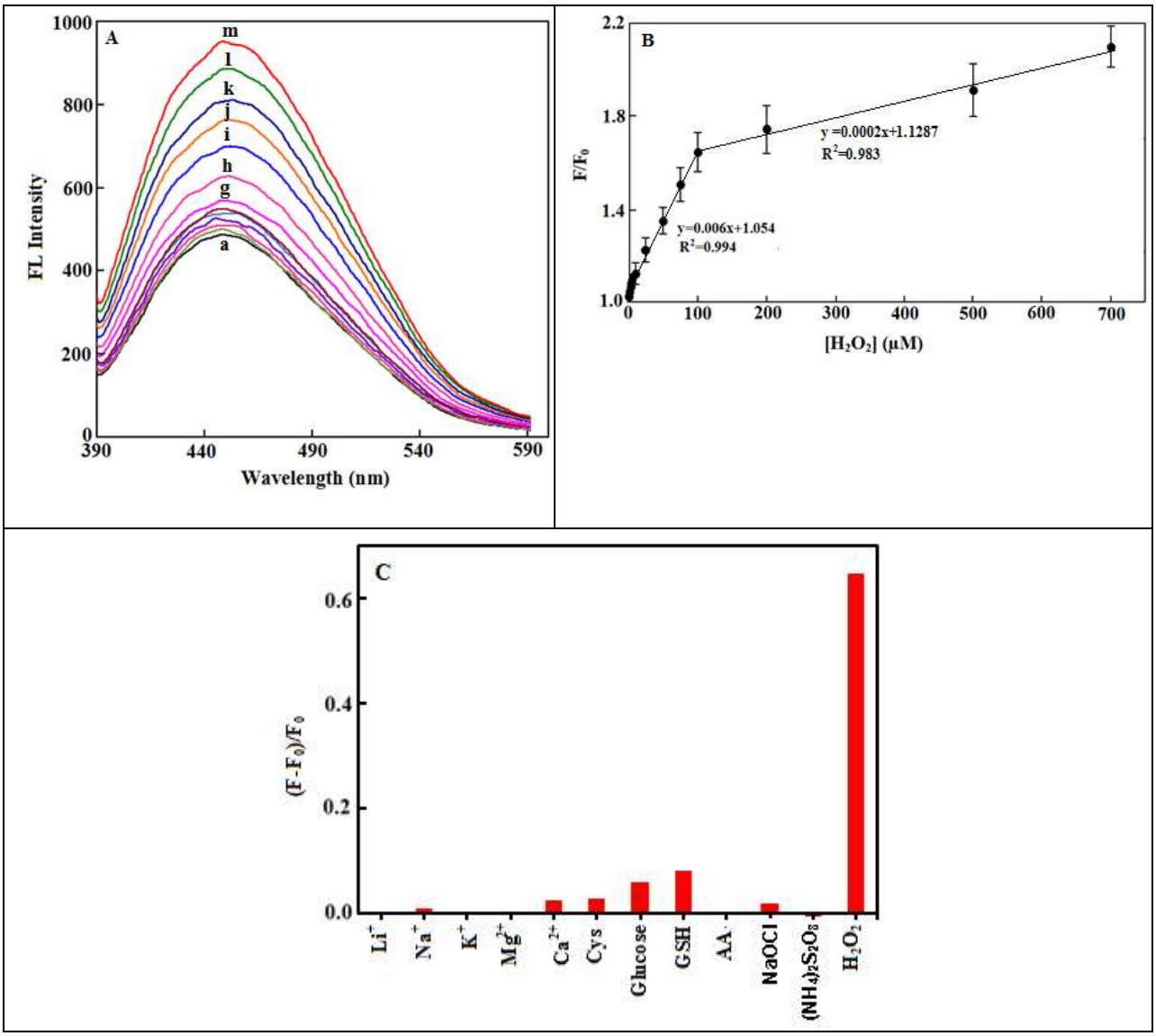

Fig. 3

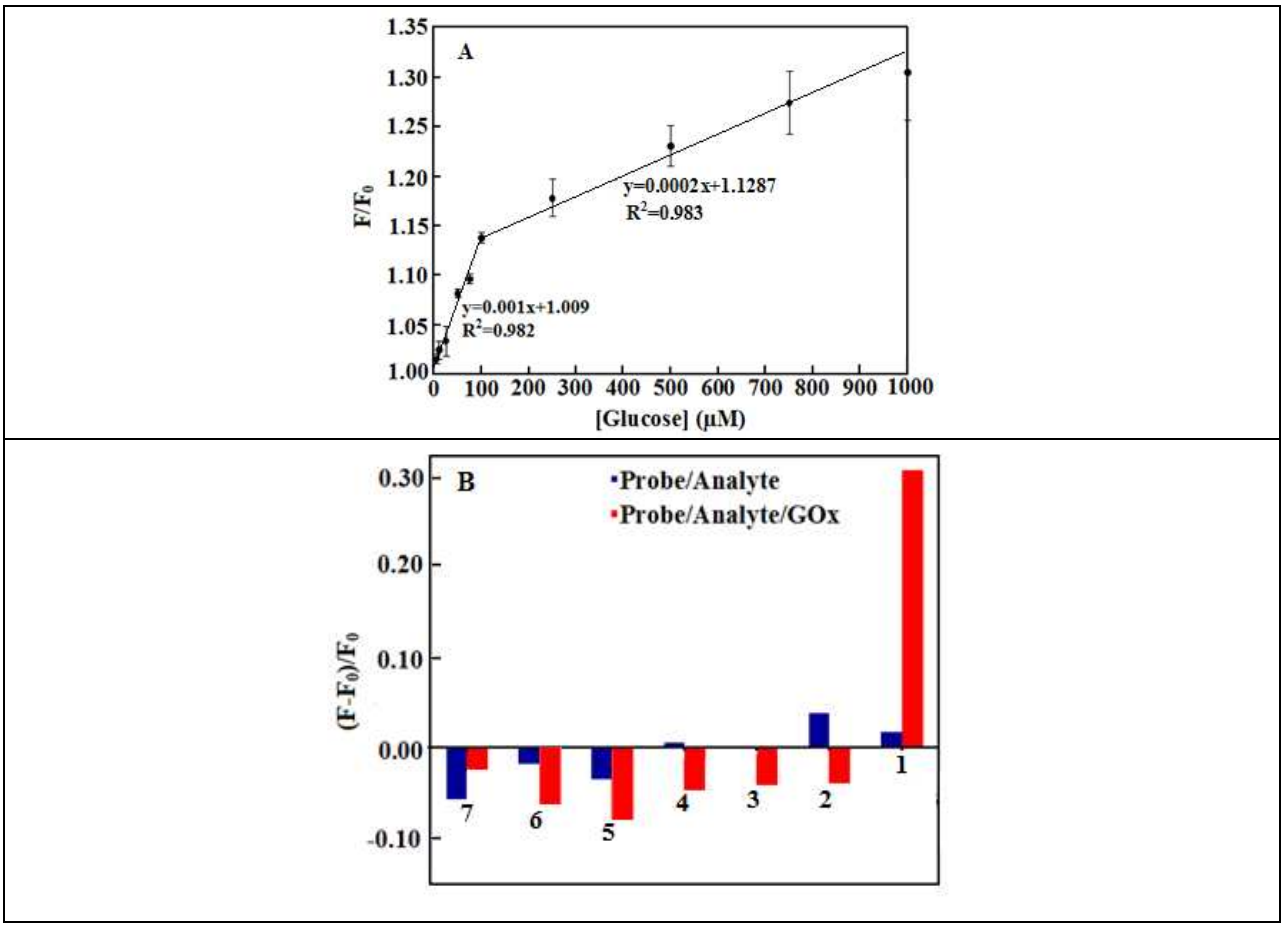

Fig. 4

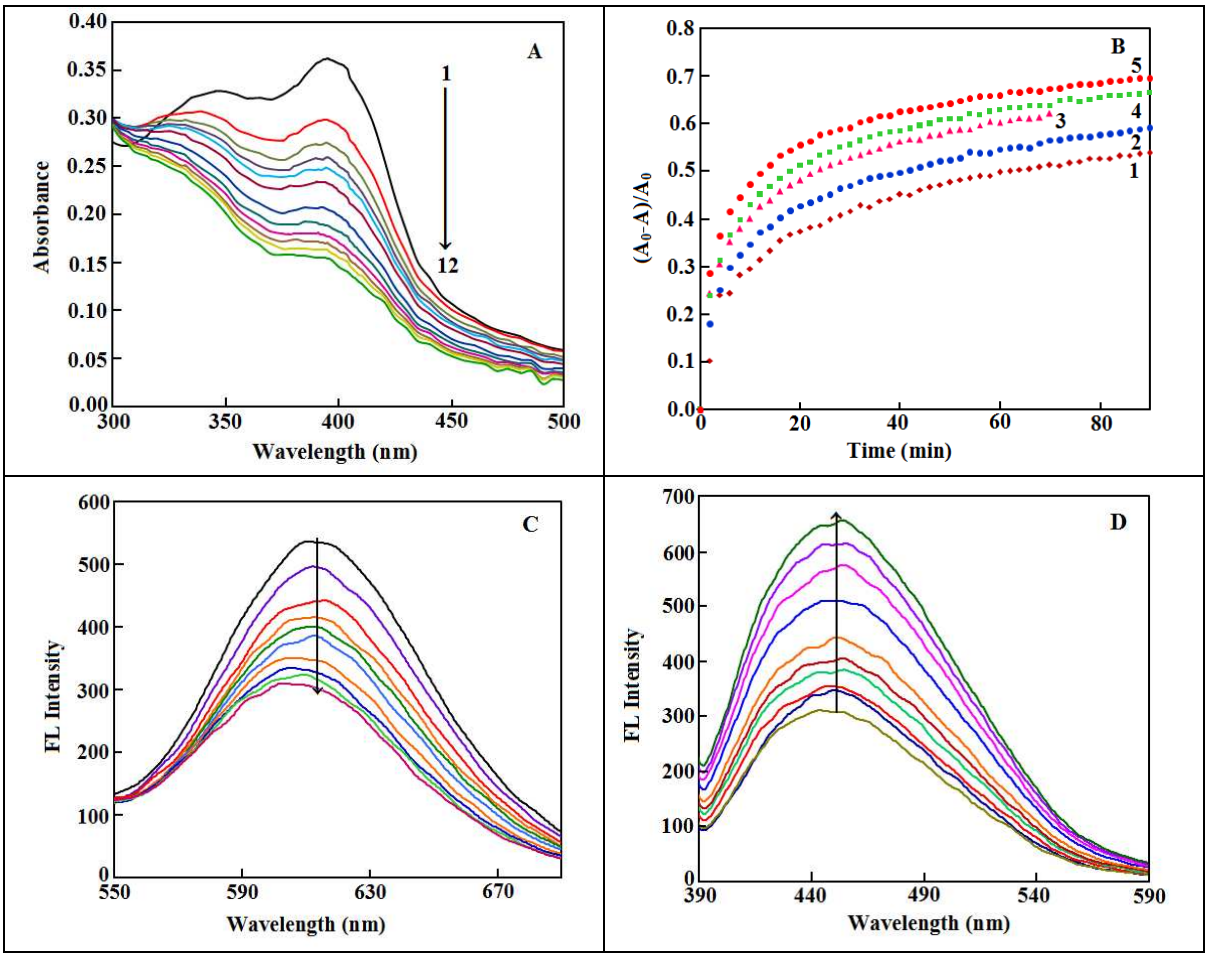

Fig. 5

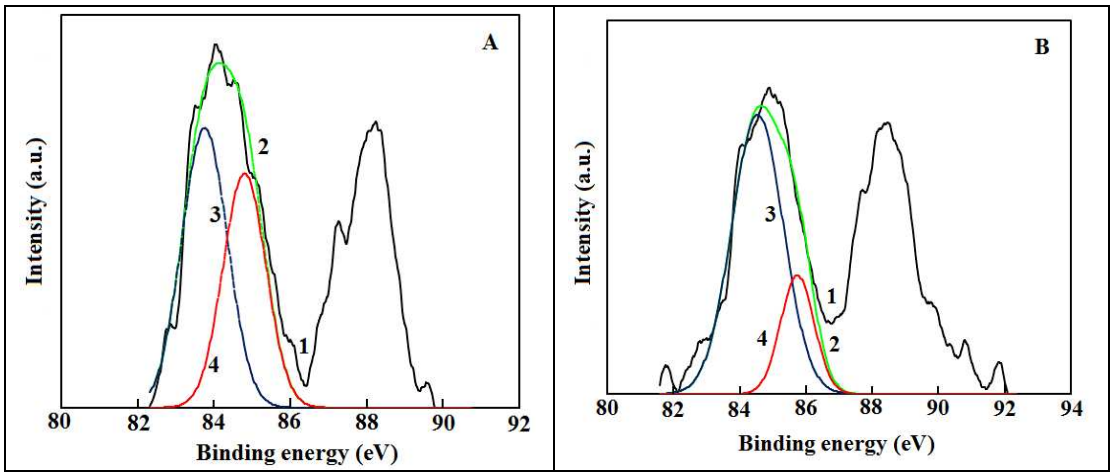

Fig. 6